background due to the secondary ions generated in the desorption process has to be corrected by either subtracting the background spectrum from the MPI mass spectrum or using a reflector to reject the directly desorbed ions in a reflectron TOFMS (*39–42*), this heating method, presumably generating neutrals for most organic compounds, will not require background correction. Another research area we are pursuing is the design and construction of a pulsed heating probe capable of varying its contact time with the sample substrate for sample vaporization. Future work will involve the use of this unique feature for the fundamental studies of the heating processes of biological molecules such as the rates of decomposition and vaporization. In addition, comparison among the pulsed heating, LD and FAB processes for the formation of neutral molecules (for instance, the studies of the intensity of the neutrals vaporized or desorbed as a function of the vaporization or desorption time) may provide some information about the heating nature of LD and FAB.

LITERATURE CITED

(1) Lubman, D. M.; Li, L. In *Lasers and Mass Spectrometry*; Lubman, D. M., Ed.; Oxford: New York, 1990; Chapter 16, pp 353–382 and references therein.
(2) Klimcak, G.; Wessel, J. E. *Anal. Chem.* **1980**, *52*, 1233.
(3) Rhodes, G.; Opsal, R. B.; Meek, J. T.; Reilly, J. P. *Anal. Chem.* **1983**, *55*, 280.
(4) Dobson, R. L. M.; D'Silva, A. P.; Weeks, S. J.; Fassel, V. A. *Anal. Chem.* **1986**, *58*, 2129.
(5) Irion, M. P.; Bowers, W. D.; Hunter, R. L.; Rowland, F. S.; McIver, R. T., Jr. *Chem. Phys. Lett.* **1982**, *93*, 375.
(6) Carlin, T. J.; Frieser, B. S. *Anal. Chem.* **1983**, *55*, 571.
(7) Sack, T. M.; McCrery, D. A.; Gross, M. L. *Anal. Chem.* **1985**, *57*, 1290.
(8) Kuo, C. H.; Beggs, C. G.; Kemper, P. R.; Bowers, M. T.; Leahy, D. J.; Zare, R. N. *Chem. Phys. Lett.* **1989**, *163*, 291.
(9) Zimmerman, J. A.; Watson, C. H.; Eyler, J. R. *Anal. Chem.* **1991**, *63*, 361.
(10) Hayes, J. M. *Chem. Rev.* **1987**, *87*, 745.
(11) Tembreull, R.; Lubman, D. M. *Anal. Chem.* **1984**, *56*, 1962.
(12) Grotemeyer, J.; Schlag, E. W. *Angew. Chem., Int. Ed. Engl.* **1988**, *27*, 447 and references therein.
(13) de Vries, M. S.; Hunziker, H. E.; Wendt, H. R. In *Lasers and Mass Spectrometry*; Lubman, D. M., Ed.; Oxford: New York, 1990; Chapter 17, pp 383–401.
(14) Li, L.; Hogg, A. M.; Wang, A. P. L.; Zhang, J. Y.; Nagra, D. S. *Anal. Chem.* **1991**, *63*, 974.
(15) Zare, R. N.; Levine, R. D. *Chem. Phys. Lett.* **1987**, *136*, 593.
(16) Hall, R. B. *J. Phys. Chem.* **1987**, *91*, 1007.
(17) van der Peyl, G. J. Q.; Isa, K.; Haverkamp, J.; Kistemaker, P. G. *Org. Mass Spectrom.* **1981**, *16*, 416.
(18) Hercules, D. M.; Day, R. J.; Balasanmugam, K.; Dang, T. A.; Li, C. P. *Anal. Chem.* **1982**, *54*, 280A.
(19) Burgess, D., Jr.; Viswanathan, R.; Hussla, I.; Stair, P. C.; Weitz, E. *J. Chem. Phys.* **1983**, *79*, 5200.
(20) Van Breemen, R. B.; Snow, M.; Cotter, R. J. *Int. J. Mass Spectrom. Ion Phys.* **1983**, *49*, 35.
(21) Beuhler, R. J.; Flanigan, E.; Greene, L. J.; Friedman, L. *Biochem. Biophys. Res. Commun.* **1972**, *46*, 1082.
(22) Beuhler, R. J.; Flanigan, E.; Greene, L. J.; Friedman, L. *J. Am. Chem. Soc.* **1974**, *96*, 3990.
(23) Beuhler, R. J.; Flanigan, E.; Greene, L. J.; Friedman, L. *Biochemistry* **1974**, *13*, 5060.
(24) Cotter, R. J.; Fenselau, C. *Biomed. Mass Spectrom.* **1979**, *6*, 287.
(25) Cotter, R. J.; *Anal. Chem.* **1980**, *52*, 1589A.
(26) Hansen, G.; Munson, B. *Anal. Chem.* **1978**, *50*, 1130.
(27) Anderson, W. R., Jr.; Frick, W.; Daves, G. D., Jr.; Barofsky, D. F.; Yamaguchi, I.; Chang, D.; Folkers, K.; Rosell, S. *Biochem. Biophys. Res. Commun.* **1977**, *78*, 372.
(28) Anderson, W. R., Jr.; Frick, W.; Daves, G. D., Jr. *J. Am. Chem. Soc.* **1978**, *100*, 1974.
(29) Daves, G. D., Jr. *Acc. Chem. Res.* **1979**, *12*, 359.
(30) Fassett, J. D.; Moore, L. J.; Shideler, R. W.; Travis, J. C. *Anal. Chem.* **1984**, *56*, 203.
(31) Wang, A. P. L.; Zhang, J. Y.; Nagra, D. S.; Li, L. *Appl. Spectrosc.* **1991**, *45*, 304.
(32) Wang, A. P. L.; Li, L. A method for Background Reduction in a Supersonic Jet/Multiphoton Ionization Reflectron Time-of-Flight Mass Spectrometer. *Appl. Spectrosc.*, in press.
(33) Sin, C. H.; Pang, H. M.; Lubman, D. M. *Anal. Instrum.* **1988**, *17*, 87.
(34) Zenobi, R.; Hahn, J. H.; Zare, R. N. *Chem. Phys. Lett.* **1988**, *150*, 361.
(35) Rizzo, T. R.; Park, Y. D.; Peteanu, L. A.; Levy, D. H. *J. Chem. Phys.* **1986**, *84*, 2534.
(36) Li, L.; Lubman, D. M. *Rapid Commun. Mass Spectrom.* **1989**, *3*, 12.
(37) Beavis, R. C.; Linder, J.; Grotemeyer, J.; Schlag, E. W. *Chem. Phys. Lett.* **1988**, *146*, 310.
(38) Li, L.; Lubman, D. M. *Anal. Chem.* **1987**, *59*, 2538.
(39) Winograd, N.; Baxter, J. P.; Kimock, F. M. *Chem. Phys. Lett.* **1982**, *88*, 581.
(40) Hrubowchak, D. M.; Ervin, M. H.; Winograd, N. *Anal. Chem.* **1991**, *63*, 225.
(41) Becker, C. H.; Gillen, K. T. *Anal. Chem.* **1984**, *56*, 1671.
(42) Pallix, J. B.; Schuhle, U.; Becker, C. H.; Huestis, D. L. *Anal. Chem.* **1989**, *61*, 805.
(43) Hahn, J. H.; Zenobi, R.; Bada, J. L.; Zare, R. N. *Science* **1988**, *239*, 1523.

Davinder S. Nagra
Jian-Yun Zhang
Liang Li*

Department of Chemistry
University of Alberta
Edmonton, Alberta, Canada T6G 2G2

RECEIVED for review April 15, 1991. Accepted July 15, 1991. This work was supported in part by the Natural Sciences and Engineering Research Council of Canada.

TECHNICAL NOTES

Improved End-Column Conductivity Detector for Capillary Zone Electrophoresis

Xiaohua Huang[1] and Richard N. Zare*

Department of Chemistry, Stanford University, Stanford, California 94305-5080

INTRODUCTION

Conductivity detection is used widely in ion chromatography (*1*) but rarely in capillary zone electrophoresis (CZE) (*2*). This difference apparently stems from the difficulty of fabricating a conductivity detector with low dead volume in the structure of a fused-silica capillary with an inside diameter at 100 μm or less. Three possible designs for a CZE conductivity detector are on-column, off-column, and end-column structures. Foret et al. (*3*) used a microscale molding method to construct an on-column conductivity detector, which was also used on-line with a UV absorbance detector. Another scheme for constructing an on-column conductivity detector employs a focused CO_2 laser beam to punch holes directly through the walls of the fused-silica capillary (*4*). Two platinum sensing electrodes are sealed on opposite sides of the column. Because CZE typically has a voltage drop of 300 V/cm along the length of the capillary, the sensing electrodes need to be aligned carefully and an isolation transformer must be used in measuring the conductance (*4*, *5*).

Off-column conductivity detectors may be constructed by grounding the capillary prior to the sensing electrode, using

[1] Present address: Department of Chemistry, University of California, Berkeley, CA 94720.

0003-2700/91/0363-2193$02.50/0

either a porous glass structure (*6*) or an on-column frit structure (*7*). Recently, Huang et al. (*8*) reported the use of an end-column structure for conductimetric and amperometric detection in CZE in which the sensing electrode is placed at the outlet of the fused-silica capillary. Such end-column detectors demonstrate sensitivities that approach those of previous on-column conductivity detectors with only a small sacrifice in resolution, an extra band broadening of approximately 25%. This end-column structure, however, requires carefully matched microplumbing, in which the analytical capillary is placed inside a second capillary that has an inside diameter slightly larger than the outside diameter of the analytical capillary.

In this paper we describe a simpler end-column conductivity detector, which we have mounted directly to the outlet of the capillary of a commercial CZE separation system (P/ACE 2000, Beckman Instruments, Inc., Palo Alto, CA). By this means, we can record both UV absorbance and conductivity during the same run. The use of both detectors provides not only greater analysis power, particularly for ions that cannot readily be detected by UV absorption, but also a calibration of the UV absorbance detector. Unlike in other CZE detection methods, conductivity shows a direct relationship between migration time and response factor (*9*, *10*). With the use of an internal standard, conductimetric detection allows an accurate determination of absolute concentrations in a mixture without separate calibrations for the response of each component. This unique advantage permits the UV absorption response to be calibrated on an absolute basis when both detectors are used together. Another advantage of a dual-detector system is the ability to determine mobilities by sensing the sample zone as it moves by two detectors located at a known, fixed distance from each other (*11*).

EXPERIMENTAL SECTION

Construction of End-Column Conductivity Detector. A small hole (approximately 40 μm in diameter) is drilled through the wall of a fused-silica capillary, 50 or 75 μm inside diameter and approximately 360 μm outside diameter (Polymicro Technologies, Phoenix, AZ) using the focused output of a home-built, computer-controlled CO_2 laser (10.6 μm, Model RF 165, Laakmann, San Juan Capistrano, CA, 40 W max). The distance from the hole to the capillary outlet is approximately 7 mm. A platinum or stainless steel 50-μm-diameter wire (California Fine Wire Co., Grover City, CA) is inserted along the length of the capillary. The tip of this wire is placed close to but not protruding into the hole structure (see Figure 1a). This wire, which serves as the sensing electrode, is sealed to the capillary outlet with epoxy adhesive (Torrseal, Varian, Lexington, MA). A fine, insulated lead wire (No. 30 wire wrap, Page Digital Electronics, Duarte, CA) is connected to the sensing electrode (see Figure 1b). Then, a protective jacket with a large hole (>1 mm in diameter) aligned with the small hole in the fused-silica capillary is attached (not shown in Figure 1). This protective jacket provides an outlet for the eluent and gives structural support. Figure 1c presents a cross-sectional view of this end-column conductivity detector. The structure is placed inside an outlet reservoir that contains the ground electrode. The ground electrode completes the electrophoretic separation circuit; the conductivity is also measured between the sensing and the ground electrodes, by using our previous home-made ac circuitry (*4*, *5*) operated at 3.5 kHz. In some studies, this end-column conductivity detector is mounted directly on the end of the capillary from the cartridge of a P/ACE 2000 unit, thereby allowing the use of dual detection, UV absorbance, and conductivity, under microprocessor control.

Reagents and Samples. All chemicals are from Sigma Chemical Corp. (St. Louis, MO) and are not further purified. Water used to prepare solutions is freshly deionized and distilled with a water purifier (Model LD-2A) coupled with a Mega-Pure Automatic Distiller (Corning Glassworks, Corning, NY). Electrolyte solutions are filtered through a 0.2-μm membrane (Acrodisc, Gelman Scientific, Inc., Ann Arbor, MI). Buffers are prepared with 2-morpholinoethanesulfonic acid (MES) and equimolar histidine (His) (3–100 mM). We also use phosphate buffer and potassium acetate buffer, with the pH adjusted as needed.

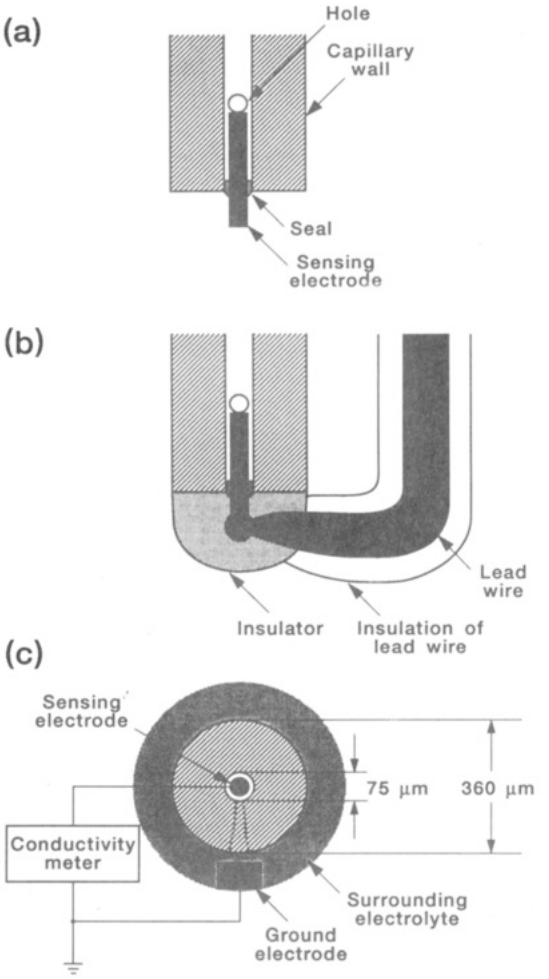

Figure 1. End-column conductivity detector: (a) alignment of sensing electrode in capillary with eluent hole in capillary wall (not to scale). (b) Same as (a) with electrical connectors. (c) Horizontal cross section. Not shown is the protective jacket, which surrounds the outlet of the capillary. Conductivity measurements are made between the sensing electrode and the ground electrode, which also acts to complete the electrophoretic circuit.

RESULTS AND DISCUSSION

Variation of Response with Placement of the Sensing Electrode. The performance of the end-column conductivity detector was examined as the position of the sensing electrode was changed relative to the eluent hole. The inlet of the capillary was immersed in a reservoir at high positive voltage (anode), and the outlet of the capillary was immersed in a reservoir at ground potential (cathode). The current through the capillary was recorded by using a current-sampling resistor (*12*). Two kinds of buffers, MES/His (10 mM, pH 6.1) and phosphate (20 mM, pH 7.0), were employed to test the low- and high-current regimes, respectively. The position of the sensing electrode was adjusted by using a microscope with a 5X objective. Four positions were studied: (1) with the tip of the sensing electrode protruding past the center of the eluent hole; (2) with the tip at the center of the eluent hole; (3) with the tip on the edge of the eluent hole, as shown in Figure 1a; (4) with the tip recessed 100 μm from the edge of the eluent hole.

For positions 1 and 2, the current fluctuated wildly after 1–2 min and then declined when high voltage (300 V/cm) was applied. We suspect that gas bubbles accumulating around the sensing electrode caused this undesirable behavior. For

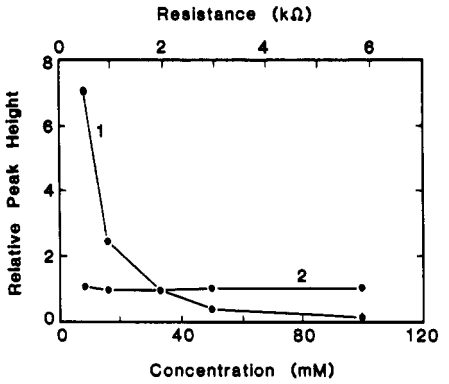

Figure 2. Plot of K^+ peak height versus MES/His electrolyte concentration. Curves 1 and 2 represent the change of the peak height with electrolyte concentration inside the capillary and inside the outlet reservoir, respectively. The K^+ peak height is measured by end-column conductance.

positions 3 and 4 the current was stable. No significant difference in current was observed between capillaries with a sensing electrode in position 3 or 4 and those with no sensing electrode. Results of a study of the electroosmotic flow rate also suggested that the sensing electrode in position 3 or 4 caused no interference in the operation of the capillary. Position 3 (shown in Figure 1a) is believed to be the optimum design because position 4 had an extra segment of liquid in front of the sensing electrode, and this liquid increased the resistance of the conductivity circuit.

Variation of Response with Differences in Electrolyte between the Capillary and the Outlet Reservoir. Recall that conductivity is measured between the sensing electrode, located inside the capillary near the capillary's outlet, and the ground electrode, located inside the outlet reservoir. An important question is whether the conductivity of the electrolyte inside the outlet reservoir affects the conductivity measured. If so, the end-column conductivity detector would respond differently from an on-column conductivity detector. We investigated how the baseline conductivity varies with the concentration of MES/His buffer in the outlet reservoir when the electrolyte inside the capillary is (a) 100 mM, (b) 50 mM, (c) 25 mM, and (d) 12.5 mM MES/His. We find that a change in the concentration of the electrolyte in the outlet reservoir hardly affects the baseline conductivity. On the other hand, the baseline conductivity changes linearly with a change in the concentration of the electrolyte inside the capillary. This study indicates that reliable conductivity measurements can be achieved without the interference of what might be called "memory effects" from sample zones that have passed by the sensing electrode. The outlet reservoir has about 1 000 000 times the volume of the capillary. Thus, the outlet reservoir serves as a giant ground electrode that is not influenced by the tiny changes of what flows into it.

Figure 2 shows the influence of electrolyte concentration (K^+ cation at 5×10^{-4} M) on peak height as the electrolyte concentration is changed in the capillary (rapidly falling curved line, denoted as 1) and in the outlet reservoir (flat line, denoted as 2). Note that a change in the electrolyte concentration inside the capillary from 100 to 5 mM causes the K^+ peak height to increase by a factor of 100, whereas the same change of electrolyte concentration in the outlet reservoir causes no detectable change in the peak height. The same behavior has been observed in CZE with an on-column conductivity detector (*13*). Figure 2 demonstrates that the present end-column conductivity detector has similar characteristics to the previously described conductivity detector (*4*, *9*).

Potential Drop between the Sensing and the Ground Electrodes. One feature that distinguishes the end-column from the on-column conductivity detector is the size of the potential drop. If the sensing electrode in the on-column detector is 5 cm from the capillary outlet, the sensing electrode is at 1500 V with respect to ground, assuming a potential of 300 V/cm. Because the sensing electrode in the end-column detector is much closer to the outlet of the capillary, the potential drop should be much smaller. We used a homemade, high-impedance dc voltage meter to measure directly the potential on the sensing electrode. We found the potential difference to be approximately 6 V under our experimental conditions (300 V/cm, 20 mM phosphate buffer, pH 7.0). Moreover, the potential drop was linear with applied electric field. A simple calculation shows that this potential drop is equivalent to measuring the potential difference to ground along a series resistor. The length of the capillary is about 35 cm and the total applied voltage is 10.5 kV; i.e., the voltage drop is 300 V/cm along the capillary, assuming a uniform bore. The distance between the sensing electrode and the ground electrode (taken as starting at the surrounding electrolyte, as shown in Figure 1c) is 0.0126 cm, where corrections have been made for the thickness of the polyimide coating that has been removed. If the hole had the same cross section as the capillary, then the voltage drop would be estimated to be 3.8 V. Actually, the cross-sectional area is less, causing the voltage drop to be larger. Our value of 6 V suggests an effective cross section of 60 μm for our capillary hole, if it were uniform. The voltage drop between the sensing electrode and the ground electrode could be lowered, if desired, by decreasing the length of this hole (using a thin-wall capillary) as well as increasing (to whatever extent possible) the cross-sectional area of this hole.

Because only a few volts difference occurs between the sensing and ground electrodes, a specially designed, isolated conductivity meter such as was used previously (*4*, *9*) is unnecessary. Instead, we use capacitors to couple the end-column conductivity detector to the ac conductivity meter. Although the voltage drop is small, it is still large enough to cause formation of gas bubbles. Evidently, bubbles are not a serious problem, perhaps because the flowing liquid suppresses build up.

Zone Broadening. We have measured the peak width of pyridoxamine by using both the UV absorbance and the end-column conductivity detector (modified P/ACE 2000 system). The UV absorbance detector was located 58 mm prior to the conductivity detector. Based on half-height measurements but with no correction for the spread of the zone with time and length, the extra zone broadening is estimated to be less than 15% for the end-column conductivity detector, based on eight separate measurements. Hence, the end-column conductivity detector introduces little loss in resolution.

A further indication of this fact is the number of theoretical plates obtained in using the end-column conductivity detector. Figure 3 shows an electropherogram of five different metal ions, each at a concentration of approximately 5×10^{-5} M (20-nL injection). This separation was not optimized; better sensitivity and higher resolution could be achieved. In this electropherogram, the Cd^{+2} cation has a peak width that corresponds to 150 000 theoretical plates.

Application of Dual-Detection Systems. Using the P/ACE 2000 system equipped with the end-column conductivity detector, we recorded both the UV absorbance and the conductance as a function of time after a sample of a complex mixture was injected (see Figure 4). The mixture included K^+, Na^+, Li^+, pyridoxamine, and the dansyl-isoleucine salt of cyclohexamine. In the UV absorbance electropherogram (Figure 4, upper trace), only pyridoxamine and dansyl-isoleucine can be identified, whereas in the conductimetric electropherogram (Figure 4, lower trace) six peaks can be

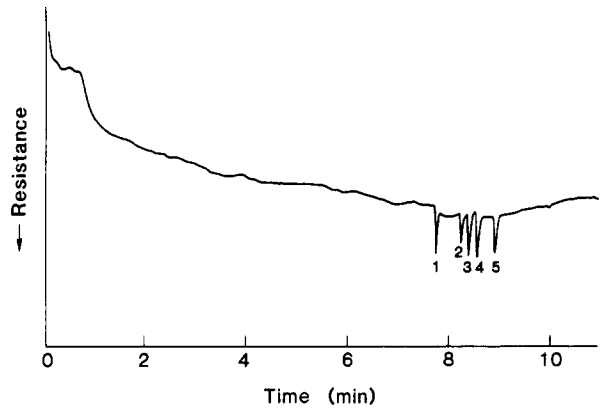

Figure 3. End-column conductimetric electropherogram for a mixture of 1 = Ca^{2+}, 2 = Na^+, 3 = Mg^{2+}, 4 = Ni^{2+}, and 5 = Cd^{2+}, about 5 × 10^{-5} M each. The running buffer is 5 mM potassium acetate, pH 5.0. The applied electric field is 200 V/cm in a 75-μm-i.d., 70-cm-long fused-silica capillary.

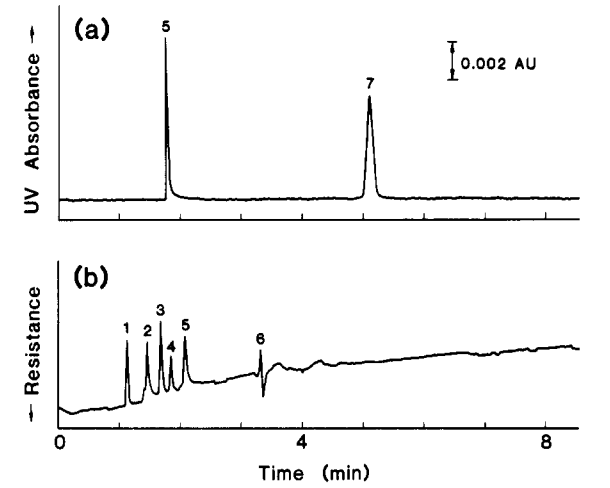

Figure 4. CZE separation of a mixture containing 1 = K^+, 2 = Na^+, 3 = Li^+, 4 = cyclohexamine, 5 = pyridoxamine, 6 = H_2O, and 7 = dansyl-isoleucine. Peaks 1-3 and 7 are ~1 × 10^{-4} M; peak 5 is 2.5 × 10^{-4} M. Peak 4 (cyclohexamine) is associated as the salt of peak 7 (dansyl-isoleucine). The upper trace is a UV absorbance electropherogram (λ = 254 nm); the lower trace is the end-column conductivity electropherogram. The running buffer is 5 mM MES/His, pH 6.0; applied voltage = 15 kV; 30 cm to the UV absorbance detector; 35.8 cm to the end-column conductivity detector; temperature = 25.0 ± 0.1 °C.

observed that correspond to K^+, Na^+, Li^+, cyclohexamine, pyridoxamine, and a water peak. These identifications were confirmed by a series of spiking experiments. Because the end-column conductivity detector is 58 mm after the UV absorbance detector, the two electropherograms are offset in time; the UV absorbance peak always precedes the conductivity peak of the same species.

Note that K^+, Na^+, Li^+, cyclohexamine, and the H_2O peak appear only in conductivity, the dansyl-isoleucine only in UV absorbance, and the pyridoxamine in both detection schemes. The dansyl-isoleucine might have been expected to be detected in conductivity, yet because MES has a similar conductivity under our operating conditions, the dansyl-isoleucine probably escapes detection by conductivity measurements. The UV absorption detector yields a nearly flat baseline, whereas the conductivity detector has a characteristic, curved baseline at early time, which reduces its sensitivity. Nevertheless, the simultaneous recording of these two different characteristics of an analyte zone can aid in the analyte's identification and quantitation.

The latter aspect deserves special mention. As pointed out previously (*9*, *10*), the use of an internal standard in CZE/conductivity detection permits quantitative analysis of the composition of a mixture without the need to make calibration curves of the detector response for the species present. Because this end-column conductivity detector is simple to construct, has small extra zone broadening, avoids epoxy adhesive near the tip of the sensing electrode, and can be operated without isolation transformers, we anticipate this detection scheme will find many uses.

ACKNOWLEDGMENT

We thank W. Howard Whitted, Beckman Instruments, Inc., for helping us attach the end-column conductivity detector to the P/ACE 2000 capillary cartridge. We are also grateful to R. T. (Skip) Huckaby, Stanford Chemistry Department, who assisted us in making the hole structure in the capillaries.

LITERATURE CITED

(1) Gjerde, D. T.; Fritz, J. S. *Ion Chromatography*, 2nd ed.; Verlag: Heidelberg, 1987. Smith, R. E. *Ion Chromatography Applications*; CRC Press: Boca Raton, FL, 1988.
(2) Kuhr, W. G. *Anal. Chem.* **1990**, *62*, 403R-414R.
(3) Foret, F.; Deml, M.; Kahle, Y.; Bocek, P. *Electrophoresis* **1986**, *7*, 430-432.
(4) Huang, X.; Pang, T.-K. J.; Gordon, M. J.; Zare, R. N. *Anal. Chem.* **1987**, *59*, 2747-2749.
(5) Everaerts, J. L.; Beckers, J. L.; Verheggen, Th. P. E. M. *Isotachophoresis, Journal of Chromatography Library 6*; Elsevier: Amsterdam, 1976.
(6) Wallingford, R. A.; Ewing, A. G. *Anal. Chem.* **1987**, *59*, 1762-1766.
(7) Huang, X.; Zare, R. N. *Anal. Chem.* **1990**, *62*, 443-446.
(8) Huang, X.; Zare, R. N.; Sloss, S.; Ewing, A. G. *Anal. Chem.* **1991**, *63*, 189-192.
(9) Huang, X.; Luckey, J. A.; Gordon, M. J.; Zare, R. N. *Anal. Chem.* **1989**, *61*, 766-770.
(10) Ackermans, M. T.; Everaerts, F. M.; Beckers, J. L. *J. Chromatogr.* **1991**, *459*, 345-355.
(11) Beckers, J. L.; Verheggen, Th. P. E. M.; Everaerts, F. M. *J. Chromatogr.* **1988**, *452*, 591-600.
(12) Huang, X.; Gordon, M. J.; Zare, R. N. *Anal. Chem.* **1988**, *60*, 1837-1838.
(13) Huang, X.; Gordon, M. J.; Zare, R. N. *J. Chromatogr.* **1989**, 480, 285-288.

RECEIVED for review April 8, 1991. Accepted July 3, 1991. Support for this work by Beckman Instruments, Inc., is gratefully acknowledged.

Surface-Enhanced Raman Spectroscopy with Abrasively Modified Fiber Optic Probes

Ken I. Mullen and Keith T. Carron*

Department of Chemistry, University of Wyoming, Laramie, Wyoming 82071-3838

INTRODUCTION

Raman spectroscopy is a very attractive technique for in situ monitoring of remote environments with optical fibers. The major advantage of Raman over its vibrational counterpart, IR spectroscopy, is the use of visible radiation. Raman can be excited with visible light, which has a high transmission in optical fibers. Furthermore, an important application of remote, optical fiber sensors is water quality analysis and water

* To whom correspondence should be sent.

0003-2700/91/0363-2196$02.50/0